LASER WELDING OF TI-NI SHAPE MEMORY ALLOY WIRE

by Young-Sik Kim[1] , Jong –Do Kim[2]

[1] Department of Mechanical and Material Engineering, Korea Maritime University

Dongsamg-dong, Yeongdo-gu, Busan, 606-791, Korea, yskim@hanara.kmaritime.ac.kr

[2] Division of Marine System Engineering, Korea Maritime University

Dongsamg-dong, Yeongdo-gu, Busan, 606-791, Korea, jdkim@hanara.kmaritime.ac.kr

ABSTRACT

Ti-50.9at%Ni wires were welded using pulsed YAG laser. The laser welded wires were tested for investigating the shape memory effect and the ability of super elasticity. The fatigue properties of the welded wires were investigated using the rotary bending fatigue tester specially designed for wires. Moreover, the effect of defocusing distance during laser welding on the static and fatigue properties was investigated.

The shape memory effect and super elasticity of the laser welded wires were approximately identical with that of base metal at the test temperature below 353K. However, the welded wires were broken within elastic limit at the test temperature above 353k. Under the cyclic bending loading conditions, the welded wires could be useful only below the elastic limit, while the base metal had sufficient fatigue life even the stress induced M-phase region. The fatigue strength of the welded wires was about half of that of the base metal. The deterioration of the static and fatigue properties in the welded wires was proven to be from the large difference of the transformation behavior between the base metal and welded part that is caused by vaporization of Ni-content at the welded part during the welding process. The defocusing distance below 3mm acted more largely on lowering the strength of the welded wires than that of 6mm or 8mm.

KEYWORDS

Pulsed YAG Laser, Super elasticity, Rotary bending fatigue tester, Defocusing distance, Stress-strain curve Martensitic transformation.

1. Introduction

The Ti-Ni shape memory alloy wires are expected as a very useful material in the fields of actuator, sensor, or medical appliance. For the promotion of practical use of that wire, it is very important to establish its welding method. Several papers have been reported about the welding method of the shape memory alloy. The gas tungsten arc welding, friction welding, resistance welding, electron beam welding, and laser welding have so far been tried to apply to the joining of a shape memory alloy[1-5]. In order to obtain the successful welded part of the shape memory alloy, it is necessary to make the heat affected zone narrow as possible[4]. The laser welding is considered to be the superior joining method of the shape memory alloy in aspect of obtaining the very narrow heat affected zone due to its high energy and high power density, and small heat input.

For making the reliable welded assembly of the shape memory alloy, the fatigue properties of the welded part must be understood. However, the welding methods of the alloy have so far been discussed based on the tensile breaking load; no works with regard to the fatigue properties have yet been conducted.

The present work was intended to apply the pulsed YAG laser welding to the joining of the Ti-Ni shape memory alloy wire. The strength of the welded wire was discussed based on the tensile breaking load and cyclic bending fatigue tests.

2. Experimental procedure

The compositions of the alloy used were Ti-50.9at%Ni. The ingots of the alloy were hot drawn, followed by cold drawn by 30% to wire of 1.0 mm diameter. The wire was cut to 100mm length for base metal specimen and to 50mm length for welded specimen. The cut wires were annealed at 673K for 3.6 ks followed by water quenching. After the heat-treatment, the specimens were polished lightly by emery papers to remove the lightly oxidized surface layer. The transformation temperatures of the prepared specimens appeared to as follows by DSC test: R*= 310K, Ms= 223K, A*= 288K, AR*= 3 13K. ARf=323K. The welded specimens were made by butt welding of the 2 wires of 50mm length using the pulsed YAG laser. The welding conditions are as follows; focal length = 150mm, defocusing distance = 3mm, 6mm, 8mm, lamp voltages = 320V, pulse length =5ms, pulse energy = 7.8J, shield gas = Ar, 301/mm. The schematic diagram of the welding process is shown in Figure 1. The welding was performed by 4 shots of the beam in the circumference of the butt joint. For avoiding the welding distortions, both base metal wires were fixed in the jig during welding process.

The shape memory effect and super elasticity for the base metal and welded specimens were evaluated using a Shimadzu Autograph AG10kND Instron type tester with a heating chamber.

Fatigue tests were carried out using a rotary bending tester which is specially designed for wires in previous work[6]. The schematic diagram of the cyclic bending fatigue test for the welded wire is shown in Figure 2. In this test, the cyclic strain amplitude can be changeable by changing the arc radius of the specimen. The tests were conducted under constant temperature, 293K and constant cyclic speed, 6.7Hz.

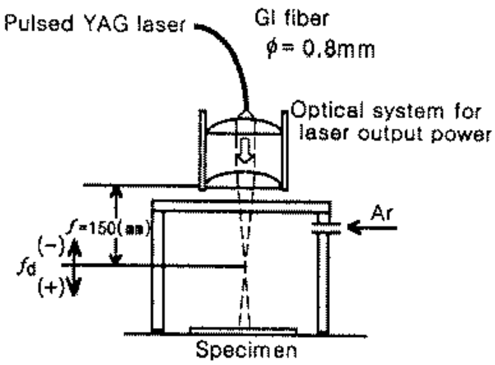

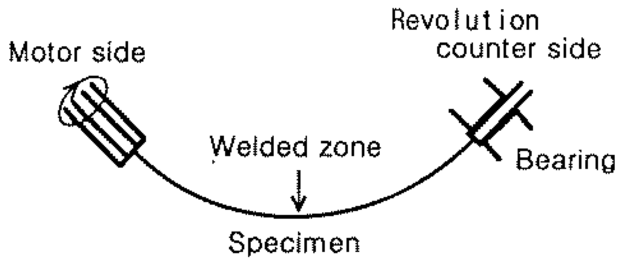

Fig. 1 Schematic diagram of the laser welding process (fd : defocusing distance)

Fig. 2 Schematic diagram of the cyclic bending fatigue test welded wire.

The transformation behaviors of the base metal and welded part were inspected by the DSC test. The functional and fatigue properties were discussed in conjunction with the change of the defocusing distance in welding process. For clarifying the reason for why the difference in fatigue life between the base metal and welded wire occurs, the transformation temperature as a function of Ni-content was investigated. Moreover, the effect of the heat treatment at 673K for 3.6 ks followed by water quenching for the welded specimens was inspected by the fatigue tests.

3. Experimental results and discussions

3.1 Functional properties of the welded wire

According to the appearance of the welded part, the welding zones showed to have a little different width with the change of the defocusing distance during the welding process. The width of the zones appeared as 1mm at the defocusing distances of the 6mm and 8mm, however, it appeared as 1.3mm at 3mm. The beam diameter increases with increasing the defocusing distance, while the energy density decreases. The appearing of the wider width at 3mm defocusing distance is considered to be from the higher energy density nevertheless smaller beam diameter.

Figure 3, 4 shows the strain- stress curves for the base metal, welded specimens with 6mm defocusing distance, respectively. The recovery strains by the heating are indicated by arrows in each diagrams. The base metal shows full shape memory effect at 263K, and it shows super elasticity at 323K and 353K. The welded specimens with 6mm defocusing distance shows nearly same behavior as base metal except somewhat lower martensite inducing stress at the temperature below 353K. Above 353K, the specimen breaks within the elastic limit. However, the welded specimen with 3mm defocusing distance showed only shape memory effect at 263K. The welded zone acts as a strain concentration part in the loading due to the change of its Ni-content during the welding process. The reason for the change of the Ni-content at welded zone will be discussed in Section 3.3. Therefore, the wider welded zone at 3mm defocusing distance leads to large strain concentrations and brings the lower strength.

The breaking within elastic limit at high temperature in the welded specimens is considered to be due to the large difference in the yield strength between the base metal and welded zone at high temperature region. The critical stress for inducing the martensite, namely yield strength in Ti-Ni alloy becomes higher with rising the

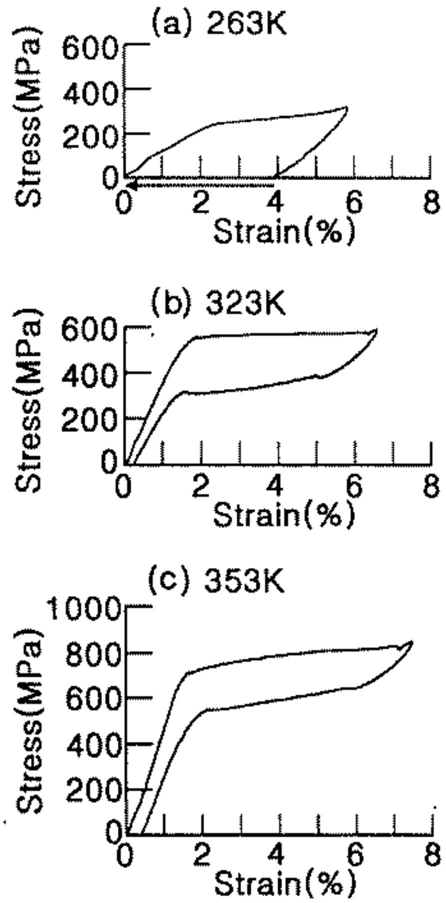

Fig. 3 Strain-stress curve for base metal .

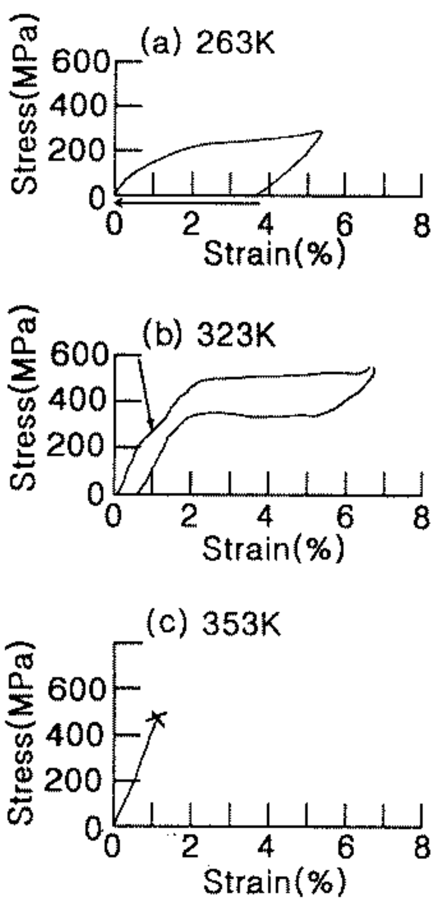

Fig. 4 Strain-stress curve of welded specimen with 6mm defocusing distance. Arrows in (b) indicates 1-step martensitic transformation.

temperature in Ti-50.9at%Ni alloy[6]. The yield strength of base metal will increase with increasing the temperature, however, that of welded zone will not increase in same rate because of its change of Ni content during welding process as above mentioned. Thus, larger difference in strength occurs at higher temperature, and leads to large stress concentration at welded zone. As the result, the welded specimen breaks within elastic limit at high temperature region.

Moreover, from the above s-s curves, it is known that the welded specimen shows the 2 step transformation behaviors even the temperature above 323K as shown by arrow in Figure 4, while the base metal shows only 1 step transformation above 323K. The 2 step transformation below 323K indicates the R-phase transformation and martensitic transformation. In general, R-phase transformation does not show in Ti-Ni alloy above 323K[7].The 2 step transformation behavior in welded specimen above 323K is considered to be caused by the separate martensitic transformation at welding zone and base metal.

3.2 Fatigue properties of the welded wire

Figure 5 shows the strain amplitude(ε_a)- number of cycles to failure(Nf) curves in the cyclic bending fatigue tests for the base metal and laser welded specimens at 293K. The welded specimens were investigated for the change of defocusing distance during welding process and the effect of the post weld heat treatment, The ε_a -Nf curve of the base metal is composed of 3 straight lines divided by 2 turning points. In previous work, the authors clarified that these turning points are coincident with the elastic limit strain and proportional limit strain, respectively[6]. This figure shows that the fatigue life of base metal is over 5G10^{3}cycles even under strain amplitude of 3.5 % which is M-phase region [see figure 3]. However, the welded specimens show 1 straight line and its fatigue life is not recognized over 1.5%strain amplitude. Moreover, the welded specimens show somewhat different fatigue life according to the defocusing distance; the 3mm defocusing distance shows a little shorter fatigue life than 6mm. This difference comes probably from the degree of strain concentration caused by the difference of the width of welding zone as mentioned in Section 3.1. Moreover, in this figure, the post weld heat treatment at 673K for 3.6 ks followed by water quenching is shown to do not affect the fatigue life. From Figure 5, it is known that the fracture strain amplitude at 2G10^{5}cycles for the welded specimens is about the half of that for base metal. Figure 6 shows the stress amplitude (σ_a)- Nf curves for the base metal and welded specimens. This curves were obtained from ε_a - Nf data by the conversion of ε_a into σ_a using the strain-

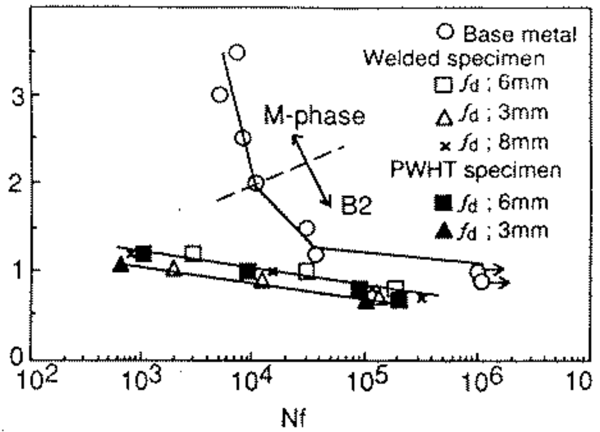

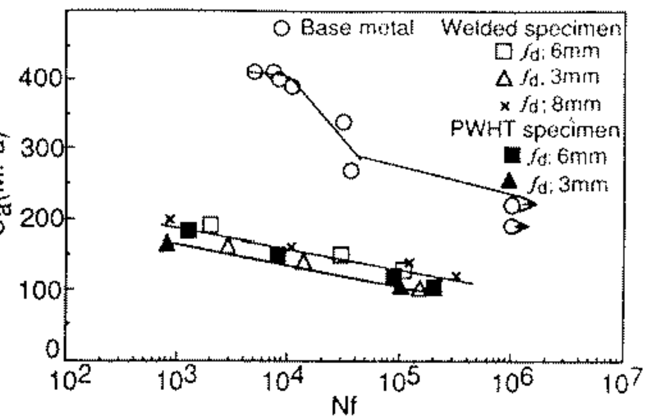

Fig. 5 Strain amplitude (ε_a)-number of cycle to failure (Nf) curves for base metal and welded specimen. (PWHT : Post Weld Heat Treatment;673K 1hr, WQ)

Fig. 6 Stress amplitude (σ_a)-Nf curves for base metal and welded specimen.

stress curve. The σ_a - Nf curve of base metal shows to be composed of 3 straight lines divided by 2 turning points, while that of welded specimens I straight line. The curves show that the fracture stress amplitude at 2G lO^{5}cycles for welded specimens is about half of that for base metal. The reason for why the difference in fatigue life between the base metal and welded specimens occurs, will be discussed in Section 3.3.

3.3 The difference in transformation behavior between the base metal and welded specimen

In order to understand the reason for why the difference in static and fatigue properties between the base metal and welded specimens occurs, the transformation behavior of the base metal and welded zone must be understood. Figure 7 shows the results of the DSC test for the base metal and weld metal. The top and bottom curves were measured during cooling and heating, respectively. The DSC curves of the base metal show two separate peaks upon cooling and heating. The peaks upon cooling correspond to the R-phase and martensitic transformation whose peak temperatures are denoted by R* and M*, respectively. The reverse transformation temperatures upon heating are denoted by A* and AR*. The corresponding Ms, As, Af, ARs and ARf points are shown in this figure. On the other hand, the weld metal shows only one peak upon cooling and heating whose temperatures are denoted by M* and A*. In the weld metal, R- phase transformation does not occur because of solution-treated effect due to the heating cycle during welding process. From Figure 7, it is known that the M* and A* point of weld metal are markedly higher than those of base metal. The M* point of weld metal shows to be 315K.

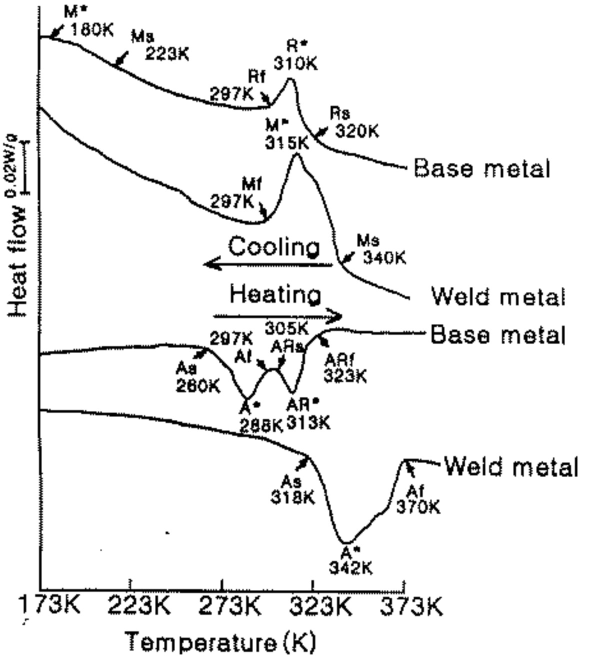

Fig.7 DSC curves for base metal and weld metal.

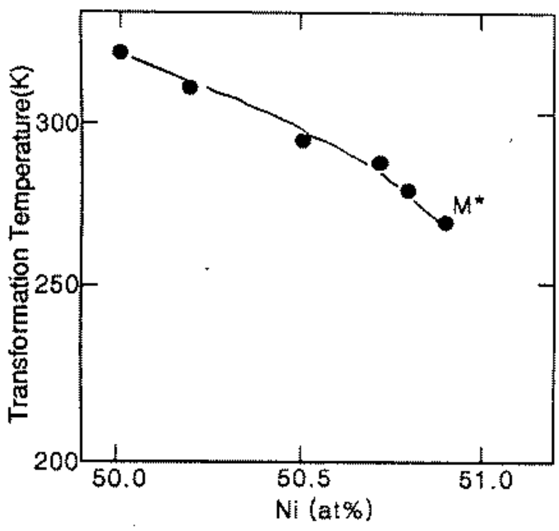

Fig.8 M points as a function of the Ni-content.

For the purpose of clarifying the reason for why the M* point rises in the weld metal, the relation between the compositions and M* point were investigated for the solution treated Ti-Ni alloy. Figure 8 shows the M* points as a function of the Ni content in the solution treated Ti-Ni binary alloy. This figure shows that the M* point rises with decreasing the Ni content. From this figure, Ni-content of M* point at 315K appears to be about 50at%. The original Ni content of the specimen was 50.9at%, and accordingly about O.9at% of Ni has disappeared; the excess Ni content evaporates during welding process. By this way, the change of the compositions occurs in the welded zone and the transformation points of welded zone become higher than that of the base metal. Besides, the weld metal softens and leads to strain concentration in the static and cyclic bending load.

From the above discussions, it is concluded that the difference in the static and fatigue properties between the base metal and welded specimens is resulted from the change of the compositions at the welded zone during the welding process. For the purpose of improving the fatigue properties of the welded wire, the solid state welding method which does not accompanying the fusion of the joining metal was recommended.

4. CONCLUSIONS

The Ti- 50.9at%Ni alloy wires were welded using the pulsed YAG laser, and the functional and fatigue properties of the welded wire were investigated for the purpose of clarifying the application of the laser welding to the joining of the shape memory alloy wire. Main results obtained are summarized as follows.

1) The laser welded wires show nearly same shape memory effect and super elasticity as the base metal at the temperature below 353K, and it shows 2 step transformation behaviors at welding zone and base metal.

2) The welded wires are broken within the elastic limit at the temperature above 353K, while the base metal shows the super elasticity.

3) Under the cyclic bending loading conditions, the welded wires are useful only within the elastic limit, while the base metal has sufficient fatigue life even the stress induced M-phase region.

4) The deterioration of the static and fatigue properties in the welded wires comes from the large difference in the transformation behavior between the base metal and welded part which is caused by vaporization of Ni-content at the welded part during the welding process.

5) The defocusing distance below 3mm in the laser welding process acts more largely on lowering the strength of the welded wires than that of 6mm or 8mm.

6) The post weld heat treatment at 673K for 3.6 ks followed by water quenching does not improve the fatigue properties of the welded wires.

REFERENCE

[1] W.J.Buehler and R.C.Wiley, United State Naval Ordnance Laboratory, NOLTR6I-75 (1961) August, 68.

[2] K.Kimura, S.Shirai, H.Tobusi and H. Iwanaga, collected papers of JSME, Vol.58. No.556 (1992) 2465.

[3] M.Makita, K.Kimura, H.Tobusi and P.H.Lin, collected papers of JSME, Vol.60, No.579 (1994) 2603.

[4] A.Hirose, M.Uchihara, T.Araki, K.Honda and M.Kondoh, J.JIM. Vol.54, No.3 (1990) 262.

[5] H.Matsuda, Master thesis,Welding Research Institute, Osaka University (1992).

[6] Y.S.Kim, T.Matsunaga and S.Miyazaki, Abstracts of JIM,No.1 19,170 (1996) 168

[7] S.Miyazaki and K.Otsuka, Metall. Trans. A, Vol.17A, Jan.(1986) 53.